

# “Metal Halide Perovskite Solar Modules: The Challenge of Upscaling and Commercializing This Technology”



Angelique M. Montgomery, Nutifafa Y. Doumon, Christa Torrence, Laura T. Schelhas, and Joshua S. Stein

## 1 Introduction

Metal halide perovskites (MHPs) are favored electronic and optoelectronic semiconductor devices due to their high conversion efficiency and low cost. In 2009, MHPs were used in the development of perovskite solar cells (PSCs) with a power conversion efficiency (PCE) of 3.8% [1]. PCE has risen rapidly to 25.7% [2] in 2022 for single-junction solar cell architectures with area < 0.1 cm<sup>2</sup>. With the current focus on low-cost, clean, and renewable energy sources, there is great interest in upscaling this technology to large-area photovoltaic (PV) modules. The Department of Energy (DOE) has defined aggressive goals to reduce the levelized cost of electricity for utility-scale PV to \$0.02/kWh by 2030 [3–5]. Two scenarios are defined to reach this goal: (1) high performance and (2) low cost. The low-cost scenario assumes module efficiency of 20% and a cost of \$0.17/W [4]. To achieve this goal, a module technology must be manufactured at a fraction of the cost of conventional crystalline silicon-based (c-Si) modules. Locally produced, solution, or

---

A. M. Montgomery (✉) · C. Torrence · J. S. Stein  
Sandia National Laboratories, Albuquerque, NM, USA  
e-mail: [ammontg@sandia.gov](mailto:ammontg@sandia.gov); [ctorrence@lanl.gov](mailto:ctorrence@lanl.gov); [jsstein@sandia.gov](mailto:jsstein@sandia.gov)

N. Y. Doumon  
National Renewable Energy Laboratory, Golden, CO, USA

Department of Materials Science and Engineering, The Pennsylvania State University,  
University Park, State College, PA, USA

Alliance for Education, Science, Engineering, and Design with Africa, The Pennsylvania  
State University, University Park, State College, PA, USA  
e-mail: [nzd5349@psu.edu](mailto:nzd5349@psu.edu)

L. T. Schelhas  
National Renewable Energy Laboratory, Golden, CO, USA  
e-mail: [laura.schelhas@nrel.gov](mailto:laura.schelhas@nrel.gov)

vapor-processed perovskite PV modules offer a promising pathway to meet this goal. However, challenges exist in upscaling from the cell level ( $<10\text{ cm}^2$ ) to the minimodule ( $>100\text{--}1000\text{ cm}^2$ ) or full module level ( $>1000\text{ cm}^2$ ); yet, current PV technologies have overcome similar challenges. While upscaling represents a significant engineering and research effort, it is a common stage in the path to commercializing new PV technologies. In this chapter we outline four critical research areas to be addressed in this path to commercialization: manufacturing, performance characterization, reliability testing, and environmental health and safety. Here, we provide a short introduction to each topic to set the stage for the development landscape.

**Manufacturing** There are many challenges to upscaling to full-sized MHP modules and developing a commercial manufacturing process. Applying uniform thin films to large areas requires fundamentally different methods than those used for small single cells. Spin coating, which is used for most small area PSC research and development, is not scalable for large areas and mass production. Instead, slot-die coating, blade coating, spray coating, or vapor-based application methods are preferred [6–17]. However, changing the film application method requires changes to the precursor ink rheology and careful attention to the processing steps and the manufacturing environment to ensure a high-quality, uniform film deposition. In addition, module fabrication involves additional processing steps compared to cells. Scribing is used between film deposition steps to divide the film into separate interconnected cells (Fig. 1a). Along with careful deposition, scribe quality and scribing precision are important aspects to module fabrication to minimize electrical losses. Another approach to using perovskites for PV modules is in a tandem structure where the PSC is placed above or below a second solar cell. The additional cell could be a variety of materials, for example, c-Si, CdTe, CIGS, organic, or even other PSCs. Monolithically integrated two-terminal (2 T) and mechanically stacked four-terminal (4 T) tandem solar cells provide a solution to the critical thermalization loss and high transmission phenomenon seen in single-junction architectures. Still, each approach faces different engineering challenges.

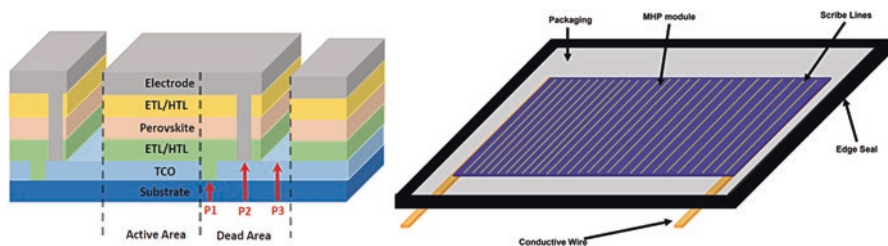


**Fig. 1** (a) Schematic for MHP thin film including all deposited layers. ETL/HTL is alternated to either an inverted *n-i-p* or planar *p-i-n* structure. This schematic includes the separation of interconnected sub-cells using scribing of P1, P2, and P3. (b) Schematic of packaged MHP module with a glass-glass configuration

**Performance Characterization** Another challenge for commercializing perovskite modules is the difficulty in characterizing module performance due to their relatively slow response and metastability. Conventional c-Si and other thin-film PV modules (e.g., CdTe and CIGS) can be characterized on the production line using a flash test, where the module is exposed to a rapid flash of light (~100 ms or less) during which an  $I$ - $V$  curve is measured. Like other current PV technologies such as CdTe and CIGS, many PSCs are metastable when initially exposed to light. Meaning their electrical output changes rapidly until it eventually stabilizes, a process that can take several seconds to hours. Preconditioning (or stabilization) is a general technique used to bring a module into a stable state so that a characterization is repeatable. Preconditioning usually involves illuminating the module until performance is stable. However, preconditioning takes time which is non-conductive for a high-speed production line that cannot wait for each module to stabilize during production. Therefore, to satisfy the unmet challenge for rapid production rates and comparable devices in MHP modules, fast measurement techniques need to be developed and validated to support high-speed manufacturing.

**Reliability** Commercial PV modules are expected to operate outdoors in varied, harsh environments for decades. A commercial thin-film module must be protected from environmental stresses such as mechanical loading, moisture, UV radiation, etc. Typically, thin-film modules are laminated between two sheets of glass to protect the active layers from the environment as shown in Fig. 1b. Perovskites are especially sensitive to moisture exposure; adding an additional packaging requirement to reduce water ingress as much as possible is preferred. Figure 1b shows a conceptual packaging design for prototype minimodules that includes double glass with an edge seal. It is important that the encapsulant material does not degrade and release reaction products that may harm the inner layers. For example, EVA, a common encapsulant material, has a degradation pathway that results in the release of acetic acid, which may degrade the MHP and corrode metal contacts [18–20]. Accelerated testing inside climate chambers can be used to provide confidence that a module can survive harsh conditions in the field. However, the applicability of current accelerated testing standards for MHP modules remains an active area of research.

**Environmental Health and Safety** Another challenge to commercialization is the fact that MHPs are made using lead (Pb) in the absorber. Most c-Si PV modules also contain lead, which is present in the solder used to connect cells together. However, there is concern that the lead in MHP is much more soluble and could be released into the environment more readily if the module were to break and be exposed to water. Early research investigated these risks using leaching tests where the module is sampled and crushed and placed in solutions of leachate. Alternative perovskite formulations with tin (Sn)-, cesium (Cs)-, and chromium (Cr)-based halide perovskites appear to be less harmful; however, the performance and stability of these alternatives are still under investigation. Alternatively, other materials can be

added to the device stack or included in the encapsulation that bind to lead and decrease transfer to the solute.

This chapter will explore these challenges among others that should be addressed before the commercialization of large-scale MHP modules can be realized.

## 2 Manufacturing of Perovskite PV Modules

There are two primary methods used to deposit the active perovskite layer and charge transporting layers (CTLs) for large-area modules: (i) solution- or chemical-based deposition (one-step or two-step) [6, 7, 21–33] and (ii) vapor-based deposition [23, 34–37]. Scalable solution methods include blade, slot-die, gravure, and spray coating. Vapor-based methods have been widely adopted in the PV industry for manufacturing CdTe PV modules [38, 39] but can require more challenging setups (e.g., vacuum processing) compared to solution processing methods.

To achieve high-performance modules, high-quality homogeneous films are required. High-quality films are often characterized by uniform coverage and pinhole-free films [33, 40]. However, achieving high-quality films for a seamless production requires a controlled manufacturing environment and atmosphere that includes posttreatments such as substrate heating [41], air-knife assistance [42], cosolvent incorporation [43, 44], antisolvent engineering [45], Lewis acid-base adduct method [46], additive engineering [47–49], and efficient precursor solution chemistries that enable low-defect solvent removal [50]. There are a number of detailed review papers on these topics and therefore will not be covered extensively here [9, 42, 46, 49, 51–72]. Precursor rheology must also be optimized for each application method and deposition technique. Multi-solvent blends are typically developed for large-area depositions to optimize film formation. Common solvents include dimethyl sulfoxide (DMSO), dimethylformamide (DMF), N-methyl-2-pyrrolidone (NMP),  $\gamma$ -butyrolactone GBL (used as cosolvent), THF, 2ME, and others. However, DMF introduces significant health risks, and GBL is subject to legal restrictions in many countries which limits their commercial viability [73]. The need for an environmentally safe nonvolatile solvent to synthesize the active and transport layers is an essential step toward commercial viability [73–77].

Green solvents exist such as ethyl acetate (EA) which is typically used as an antisolvent for perovskite precursor to optimize the perovskite/transporting material interface [78]. However, EA evaporation is slow and could impact the active layer crystallization process [78, 79]. Therefore, developing new green solvent chemistries with more volatile systems are needed for low-energy, low-cost scalable fabrication methods with limited waste and efficient precursor chemistries for large-area manufacturing [61, 74, 75, 77–82].

To make modules, it is necessary to add scribing steps between the deposition of the various layers of the perovskite device (Fig. 1a). The division of the film into separate smaller series-connected sub-cells increases the voltage; however, the

current in the module is limited by the lowest current produced by any of the sub-cells. Therefore, reducing resistive losses and increasing efficiency are dependent on developing homogeneous deposition processes for all functional layers.

Scribing techniques used within the literature rely on three scribing steps P1, P2, and P3. The scribing is repeated depending on the number of sub-cells on a single large-area substrate. P1 patterning defines the width of a sub-cell and isolates the substrate from the front transparent conductive oxide (TCO) layer. After the deposition of the electron/hole transporting layers as well as the absorber layer, P2 scribing is performed. An interconnection of the neighboring sub-cells is produced by selectively removing the top layers of the oxide to expose the TCO layer with mechanical or laser scribing. The precision of the P2 scribe is very important because it is used to establish a series contact between the back and front conductive layers of neighboring cells in the module to ensure optimum charge conductivity [83–85]. If P2 is not precise, the current transport that is formed from the electrical interconnection of sub-cells is limited [32, 84, 86]. The final P3 scribe is performed after the application of the bottom electrode which completes the monolithic series interconnection by producing electrical isolation for the top electrode and the adjacent sub-cells. The bottom electrode is laser scribed to electrically disconnect the back contact from sub-cells to form P3. The region between P1 and P3 is considered the “dead area” because it does not contribute to PV conversion under operational conditions [86, 87]. Scribing methods must be precise, and the purpose of scribing is to achieve good electrical series interconnection with low active area loss. Efficient scribe passivation and a good electrical series interconnection with very low area loss is key for high-performing modules. As more research pivots to the module scale, scribing and passivation will likely become a critical focus of the research community.

Inactive area losses are defined by the geometrical fill factor (GFF): the ratio between active area and total area [88]. By enlarging the module area, the GFF can be enhanced because the ratio of dead area associated with edges for encapsulation and frames is reduced [88, 89]. However, as active area width is lost, the photogenerated carriers are reduced and the efficiency suffers. Therefore, there exists a trade-off between wider cells (lower inactive area with higher resistive losses) and narrower cells (higher inactive area and lower resistive losses) [90, 91]. It is for these reasons that there is still a significant gap between cell and module efficiencies. Panasonic Corporation achieved a PCE of 16.09% for a perovskite module with an aperture area of 802 cm<sup>2</sup> which is 30 cm long, 30 cm wide, and 2 mm thick [92].

The need for a reliable low-cost manufacturing process depends on a reproducible method with high-throughput homogeneous deposition. Roll-to-roll and sheet-to-sheet processing are attractive options for MHP manufacturing. Roll-to-roll is a low-cost operation that allows for flexible substrates, continuous production, and high speeds [93–95]. Sheet-to-sheet processing is less susceptible to damage than roll-to-roll; however, switching to multiple substrates is easier in this method because there is only one roll holder [94, 96]. In either system, reproducibility is

critical with large-area substrates to ensure the manufacturing process yields similar performance properties every time.

Careful characterization and rapid production rates for large-area MHP modules are contingent upon the quality and efficiency in module performance characterization and in-process characterization methods that reflect the unique behavior of MHP. Multiple steps within perovskite module production will rely on fast and efficient in-line characterization methods to validate module performance and identify key parameters that impact production quality for a highly controlled manufacturing process.

### 3 Performance Characterization

To produce high-quality MHP modules, process control and in-line detection methods that quickly monitor the film quality and performance of modules are needed. Performance loss under illumination is identified depending on its effects in the current–voltage ( $I$ – $V$ ) characteristics of the device [97–99]. Electronic shunts, ohmic loss (voltage drop), recombination loss, and reduced current generation all impact device performance [97]; however, most are manufacturing defects that can be improved with careful large-scale fabrication. MHP undergoes voltage changes when exposed to light and voltage bias with rates affected by temperature. Therefore, fast measurements to monitor the film quality and its electrical characteristics during multiple stages of production are critical to ensure long-term performance for project owners and investors.

Small electronic shunts originate from high resistance between the cell's two contacts that cause local heating (hot spots) and faults that influence hysteresis behavior and reduce the maximum power [100]. Uneven coverage of the absorber and contacts, inhomogeneities between the deposited layers, and rough surfaces can cause shunts that impede the current generation and performance parameters like  $V_{oc}$  and FF. As a result, power is reduced, and an undesirable  $I$ – $V$  hysteresis may result which is mainly related to ion migration in the bulk and at the interface of the device [101–103].  $I$ – $V$  curves and electroluminescence (EL) imaging are typically used to monitor shunt behavior at various stages of production.

The PV community reports device performance at a fixed condition, known as standard testing conditions (STC). This is defined as a module temperature of 25 °C, solar irradiance of 1000 W/m<sup>2</sup>, and a reference spectrum defined at air mass of AM1.5 [104]. STC creates uniformity in testing conditions for accurate comparisons of module performance from different manufacturers. In an  $I$ – $V$  measurement, a voltage is swept across a device, and the current is recorded at each stabilized voltage step which typically takes seconds [104]. Ideally, the measured current will be dependent on the measuring conditions (voltage, temperature, irradiance, environmental conditions) and not the prior history of the device [104]. However, perovskites response times (seconds to minutes) require longer sweep times and scan rates to allow for sufficient current stabilization at each voltage step [93]. The

IEC 60904-1 measurement standard describes procedures for  $I$ - $V$  characteristics of PV devices to ensure basic requirements for  $I$ - $V$  measurements, define procedures for different measuring techniques, and include practices to minimize measurement uncertainty [105]. However, the IEC 60904-1 standard does not describe the special treatments needed to stabilize the current before performance characterization. Characterization methods typically use simple equipment; however, due to MHP metastability and slow responding device behavior, precise measurements require specialized equipment and expertise.

The primary measurement used to rate modules during production is the maximum output power ( $P_{\max}$ ) ratings at STC. This is an essential parameter for accurate output power rating nameplates and specification data sheets that distinguish between cost-dependent high-performing and low-performing perovskite modules. The higher the power rating, the more watts the module produces and the more expensive the module. Power ratings are critical because they aim to match real-life conditions for a fair understanding about how modules perform outdoors. However, accurate  $P_{\max}$  is a challenge because it is difficult for a simulator to exhibit real environmental conditions by only varying the temperature and irradiance without the consideration of environmental stressors. Maximum power point (MPP) tracking is a continuous steady-state measurement to find the maximum power by using a perturb-and-observe algorithm to keep the device at its maximum power for some time, and then an average power is reported to represent  $P_{\max}$ .

Flash tests are a quick method that can be automated on a production line and performed approximately at a rate of once per second by exposing the module to a fast (20–100+ ms) flash of light during which an  $I$ - $V$  curve is produced and  $P_{\max}$  is measured. Flash tests are a conventional method used to yield power ratings for current commercial PV technologies. Spectral uniformity match, spatial uniformity, and temporal stability are used to assess the reliability and quality of the measurement. It is performed several times during production, especially after lamination to test the functionality and performance of the completed module. Though flash testing has shown its effectiveness for current commercial PV technologies, it remains a challenge for MHP modules. Song et al. showed that fast  $I$ - $V$  curves may overestimate  $I_{\text{sc}}$  and underestimate FF for PSCs compared to a slow asymptotic continuous scan [94, 106–108]. Increasing the scan speed is possible for a flash test; however, it could overestimate performance parameters like  $V_{\text{oc}}$ . Decreasing the scan speed could easily give time for carrier generation and extraction to come to completion; however, slow scans require different light source and increase the overall testing time. It is difficult to assume that all identical modules will respond identically to a flash test, though this test could give a close enough approximation to a consistent performance measurement to distinguish between best- and worst-performing modules. This is an area of current research.

Dynamic  $I$ - $V$  or asymptotic  $I$ - $V$  measurements are like conventional  $I$ - $V$  in which a stepwise  $I$ - $V$  is produced; however, at each voltage step, a stabilization period allows the device under test (DUT) sufficient time to complete current collection. Essentially it is a series of stabilized current at fixed voltage (SCFV) measurements over a specific voltage range.



Some MHP cells and modules exhibit different  $I$ - $V$  behavior depending on the direction of the  $I$ - $V$  curve ( $I_{sc}$  to  $V_{oc}$  vs.  $V_{oc}$  to  $I_{sc}$ ) [52]. This  $I$ - $V$  hysteresis behavior is dependent on parameters such as scan rate, scan direction, bias applied, preconditioning, and device architecture [101, 109–111]. Different electrical characteristics of an  $I$ - $V$  curve limit reproducibility and lower carrier mobility and collection rates while presenting challenges for a fast-responding stable measurement. The origin of an  $I$ - $V$  hysteresis is mainly ion migration; however, ferroelectric polarization, ion trapping, and capacitive effects are also potential causes [102, 106, 107, 112–116]. Ion migration in MHP gained much attention when Snaith et al. suggested that it was one of three possible origins for the  $I$ - $V$  hysteresis phenomenon and showed how device architecture and process control influence the severity of the  $I$ - $V$  hysteresis behavior [117–119]. They showed that a stabilized power output is possible under operational conditions; however, the  $I$ - $V$  hysteresis is likely to affect MPP tracking effectiveness. More work in this area should focus on ion migration kinetics and how light illumination and dark storage impact the movement of ionic and electronic species and device stability.

The effect of operating temperature on module performance is an important parameter for yield assessment. Not many studies have been performed to measure these effects on PSCs or MHP modules. Moot et al. studied PSC performance with temperature and found the relationship to be nonlinear [120]. They showed that efficiency vs. temperature for MHPs was influenced by a change in  $V_{oc}$  and  $I_{sc}$  which is distinct from c-Si which is predominantly affected by  $V_{oc}$  [120, 121]. Accurate temperature coefficient calculations are necessary for the commercialization of this technology. More work is needed in this area.

## 4 Reliability

This section discusses degradation, stability, lifetime, durability, and reliability of MHP modules. Though these terms may seem similar, they have only one thing in common: they are all affected by the degradation mechanisms at the individual cell level and/or the failure modes at the module level. Degradation is the observed deterioration of PV performance parameters due to different stressors resulting from chemical or mechanical effects. Stability is the investigation of the degradation and the mechanisms behind this phenomenon to determine how fast or slow the process occurs over time [122]. The lifetime of a cell or module is how long (in minutes, hours, or years) the cell or module produces power at a reasonable level in a safe manner [123]. The lifetime is usually defined as the time it takes the cell or module to lose 20% or retain 80% of its initial power, often referred to as  $T_{80}$  [122, 124–127]. While durability focuses on maintaining output power level of cell or module, reliability focuses on the module's failure [123]. Using our definitions, a MHP technology would be said to be reliable if it performs a specific function for the expected lifetime. On the other hand, it would be durable if it can withstand pressure, wear, or damage while performing its function.



Degradation sources in PV can be generally classified into intrinsic or extrinsic, interfacial, or a bulk device effect. Module failure modes include other external factors, in addition to the individual cell's degradation sources, such as environmental stressors (e.g., wind, UV) and damage to the PV module themselves. The intrinsic degradation of the bulk active layer of the MHP cell can be caused by several stressors resulting in photooxidative degradation [125, 126, 128, 129], thermal degradation [126, 130], general degradation due to morphological changes or heterogeneity of the active film [130–132], and/or interface degradation [126, 132, 133]. The most influential factors in the intrinsic MHP degradation pathways could be (i) diffusion of oxygen ( $O_2$ ) and/or moisture causing oxidative degradation of the active layer, delamination, interlayer reactions, and/or oxidation of electrodes [128, 129, 134–136]; (ii) temperature effects or heating leading to thermal degradation, pronounced degradation due to thin-film heterogeneity, and/or metal ion diffusion [128, 130, 134, 135, 137, 138]; and (iii) UV-light responsible for light-assisted doping by  $O_2$  and/or photo-induced degradation [129, 132, 134–136]. All three degradation pathways can occur simultaneously in cells and modules. However, in modules there could be additional failure modes due to interconnections and packaging. The performance stability and lifetime measurements of laboratory-scale next-generation PVs including MHP PVs (with specific challenges known to MHP module fabrication) have so far only been limited to a couple of hundreds to thousands of hours [100, 125–127, 139]. However, for the levelized cost of energy metrics to approach SETO's 2030 goal of \$0.02/kWh, MHP modules are expected to last at least 20 years in the field [3]. It is worth noting that groups are exploring avenues for shorter lifetime modules, leveraging recycling, repair, and repowering approaches.

Any number of stressors, defects, or environmental conditions can lead to module failure modes and therefore lead to low module reliability and durability. This is equally true for traditional PV technologies like c-Si or CdTe. Here, we classify these degradation modes generally into two groups based on whether they are visually observable or not. Table 1 shows the detailed classification and some of the tests (discussed later) needed to certify or qualify the modules for field operation. Getting a deeper understanding of the various degradation, defects, and failure modes at the fundamental level, both quantitatively and qualitatively, is essential for advancing the technology. It will be crucial for developing qualification and safety test protocols unique to MHP modules. This is a task currently undertaken by one of SETO's funded joint projects under the Perovskite PV Accelerator for Commercializing Technology (PACT). PACT's protocols are under development and updated regularly [140].

#### **4.1 Qualification and Safety Testing**

Since much of the current MHP research has been at the lab and cell level, many researchers use the protocols set under the international summit on organic photovoltaic stability (ISOS) [4, 66]. The ISOS protocols are not meant as a replacement

**Table 1** Identified degradation mechanisms and failure modes in MHP PV cells and modules

Visual defects	PV cells within the module	PV module	Environmental factors
<b>Yes</b>	<ul style="list-style-type: none"> <li>·Cracks/fracture</li> <li>·Edge seal defects</li> <li>·Corrosion of cell metallization</li> </ul>	<ul style="list-style-type: none"> <li>·Damages to frame and junction box</li> <li>·Corrosion and breakage of glass</li> <li>·Discoloration and delamination (or degradation of back sheet)</li> <li>·Sealant issues/defects</li> <li>·Discoloration and delamination of encapsulant (degradation of encapsulant)</li> <li>·Cracks/fracture</li> <li>·Electrical arcing</li> </ul>	<ul style="list-style-type: none"> <li>·Shading</li> <li>·Soiling</li> <li>·Structural failures due to natural events (rain, sun, wind, snow, hail, fire, dust, etc.)</li> </ul>
<b>No</b>	<ul style="list-style-type: none"> <li>·Light-induced degradation</li> <li>·Light and elevated temperature-induced degradation</li> <li>·Potential-induced degradation</li> <li>·Edge deletion</li> <li>·Thermal degradation</li> <li>·Cracking and mechanical delamination of MHP layers (Fig. 1a)</li> <li>·Shunts due to laser scribing and impurities in the MHP thin film</li> </ul>	<ul style="list-style-type: none"> <li>·Contact failure due to electrochemical corrosion between MHP films and metal electrodes</li> <li>·Internal circuitry discoloration</li> <li>·Breaks in electrical circuitry</li> <li>·Substring in open circuit</li> <li>·Nonfunctioning bypass diodes</li> <li>·Thermal degradation</li> <li>·Cracking and mechanical delamination of MHP cell layers (Fig. 1a)</li> <li>·Failure of electrical solder bond</li> <li>·Reversed bias hot spots</li> </ul>	<ul style="list-style-type: none"> <li>·Reverse-biased degradation due to shading on cells connected in series</li> <li>·Degradation due to natural events (rain, sun, wind, snow, hail, fire, dust, etc.) such as moisture permeation or thermal fatigue</li> </ul>

for qualification testing; rather they are to be used as research tools. Researchers and manufacturers follow certain standard protocols to assess how well a module would perform under stressors. We refer to these as accelerated stress tests (ASTs).

At the industry level, a set of ASTs are used to similarly assess any type of PV module. They are qualification testing or type approval testing (in other parts of the world) and safety testing. Passing both qualification and safety testing is a major step in commercializing a PV module. Qualification testing, a set of defined ASTs, is usually derived from a reliability testing program. They are set by the International Electrochemical Commission (IEC) to determine the module quality. In other words, it consists of various module quality tests (MQT) that include application of one or more stressors for a prescribed length of time. Tests are pass/fail with different criteria defined for each MQT. They help detect early known degradation or failure modes of PV modules in particular environments with limitation in duration of test, acceptable costs, and level of quality of individual modules that pass the test.

The qualification testing is a blank pass or fail process, and therefore these tests do not determine a module’s entire lifespan.

In today’s PV module technologies, there are three such qualification tests depending on the type of PV modules to be tested, either c-Si PV, thin-film PV modules such as a-Si or CdTe, or concentrator PV modules. They are known, respectively, as the IEC 61215, IEC 61646, and IEC 62108 protocols [141]. These standards are revised and improved over time, with the intent of ensuring a rigorous AST standard consistent with reproducible environmental stressors such as temperature, light, and humidity. For instance, the first qualification testing for terrestrial PV modules, the IEC 61215 protocol, was established in 1993. Its third edition, revealed in 2016, has merged IEC 61215 and IEC 61646 protocols, bringing significant changes to the technical content with the inclusion of light exposure, specific to each technology.

Today’s qualification tests are a result of the 1975 US government’s efforts to improve PV module performance, leading to the jet propulsion laboratory (JPL) block buy program. Modules were designed and produced under contracts by different manufacturers, tested in phases—the block buys—and labeled as Block I to V [142]. The blocks were run through a series of ASTs intended to reproduce field-observed failures. These tests were adapted over time as modules designed were optimized until the modules were discontinued or successfully passed the qualification testing. Details of the blocks by modules and qualification testing can be found in Ref. [142]. Consequently, the PV community does not have to fully reinvent the wheel for MHP module qualification testing. We can take clues and acquired knowledge from the JPL program, learning from it and constantly applying modified versions based on our evolving understanding and insights into MHP module degradation and failure modes.

The other standard test type is safety testing, offered under the IEC 61730 or Underwriters Laboratories (UL 61730). Both tests focus on safety and nonhazardous operation of the PV modules [143]. Currently, there are two protocol versions for the safety testing for the IEC 61730 standard, namely, IEC 61730-1 and the redline version, IEC 61730-2. The safety test demands that fundamental PV module construction requirements are met to provide safe fire, mechanical, and electrical functioning of the modules over their lifetime. It consists of various module safety tests ( $MST_i$ ), in total around 56 ( $0 < i < 57$ , with  $i$  a natural number) under the IEC 61730-2 protocol requirements. They are important, as they seek to help prevent, during the operation of the modules, personal injuries due to environmental and mechanical hazards, fire hazards, and electrical shocks. The safety concerns and testing for MHP PV modules may have to go beyond the current parameters and consider other environmental and health hazards (i.e., possible leaking of Pb into the surrounding environment of the modules) as discussed in Sect. 15.5.

The current IEC standards for testing are tailored for commercially available PV technologies, with c-Si and a-Si being the baseline. Thus, these tests are unlikely to fully capture and consider all the prevalent failure/degradation modes of the next-generation thin-film PV modules such as MHPs. As indicated, MHP degradation/failure modes are governed by multiple factors that affect the device’s long-term

stability, still not fully understood (still under discovery due to differences in materials), and thus may not be well appreciated by the IEC standards. For example, improvements to MHP materials and devices have increased thermal stability, but exposure to light at elevated temperature remains a critical stressor to determine durability. Currently, there is not a light and elevated temperature test as part of the IEC-61215 tests. In addition, existing IEC tests may need to be fine-tuned for the next-generation thin-film modules, especially MHP modules, as the current tests may also cause other failure modes otherwise not observed in the field [144].

Advancing the long-term performance stability of these new technologies is crucial to their commercialization and deployment. However, even at the lab scale, there are a lot of inconsistencies in reported procedures and parameters [126, 145, 146]. For these reasons, some members of the MHP PV community came together to lay down some ground rules based on the ISOS protocols [124, 126] in what came to be known, especially for MHP, as the “consensus statement for stability assessment and reporting for perovskite photovoltaics based on ISOS procedures” [126]. These ground rules guide laboratory-scale research testing, as they are more focused on the MHP devices at the cell level. In addition, SETO went a step further, publishing minimum requirements for durability/reliability performance targets, using modified IEC 61215 protocols combined with the ISOS-L-2 light soaking test [126] of the ISOS protocols, as a baseline for meaningful assessment of MHP module scale qualification testing until an international AST standard is reached. While the details of the ISOS-L-2 and other protocols for lab-scale next-generation PV cells can be found in Ref. [126], SETO’s recommended MQT from IEC 61215 comprises of (i) MQT<sub>10</sub>, UV preconditioning; (ii) MQT<sub>11</sub>, thermal cycling; (iii) MQT<sub>13</sub>, damp heat; and (iv) MQT<sub>21</sub> PID [3]. This set of tests does not consider the humidity freeze test (MQT<sub>12</sub>) and others, as SETO’s focus is on the material and device stability rather than the packaging. It is our opinion that any AST standard considering packaged MHP modules for commercial viability should eventually include all other relevant MQT tests, but this is a good starting point for the technology. Another simple but crucial quality test not mentioned in the SETO recommendation is the electroluminescence (EL) test, capable of unearthing otherwise invisible microscopic defects such as cracks, moisture effects, and welding issues.

One risk with ASTs is the possibility that they will produce degradation not consistent with outdoor field performance. Ideally, ASTs do not reveal degradation that is not observed in real-world operation. Thus, one must always reconcile these differences by quantitatively and qualitatively comparing the outcome of the two tests. These comparisons may help fine-tune the ASTs over time and can be used to improve the IEC protocols. This approach can be used to develop tests that would be acceptable for MHP modules and packaging qualification and safety testing. A critical component to this test development will be field testing of MHP modules in the field in different climate zones (to cover the specificities of the different climate zones in the final international standard protocols). For example, such an effort combining AST and outdoor field performance of Si PV modules is already underway, led by the national renewable laboratory under the Durable Module Materials (DuraMAT) consortium [147]. They focus on accelerating the development and

deployment of durable and high-performance materials for PV module packaging to increase field lifetime and lower the cost of solar-generated electricity. This same approach could be applied to MHP modules to assess the viability of current test protocols and/or inform modifications to the test procedures.

In brief, for reliability and durability testing of PV modules, international standard tests are readily available for module qualification and safety testing. However, these tests may have to be amended, updated, or adjusted to properly validate the next-generation thin-film PV modules, such as MHP modules. It requires that novel approaches to AST protocols attuned to these technologies be explored to, if needed, adequately update the current standards and successfully qualify the next generation of PV modules. Some works are underway, namely, the ISOS consensus at lab scale and SETO's DuraMAT and PACT projects for developing materials and protocols for the module's reliability and durability.

## 5 Environmental and Health Risks

Most well-performing, highly efficient MHP modules/cells contain a soluble form of lead in the absorber layer which poses environmental and health risks. Tin (Sn), cesium (Cs), and chromium (Cr) show potential for a lead-free alternative; however, these semiconductor material combinations do not perform as well as lead-based semiconductors [148]. In addition, solvents used for precursor fabrication have toxicity risks, but these solvents are essential for the crystallization, nucleation, and growth dynamics of the MHP film. Worker safety regulations help to minimize exposure to workers through indigestion, inhalation, or skin contact. It is important to understand the health risks of MHP PV from its production to its final disposal and examine materials, processes, and unplanned events that can affect its safety.

When exposed to moisture, lead halide perovskites will degrade and ultimately form lead iodide ( $\text{PbI}_2$ ).  $\text{PbI}_2$  is highly soluble with a solubility constant ( $K_{\text{sp}}$ ) in the range of  $8.3 \times 10^{-9}$  to  $1.84 \times 10^{-8}$  [149–151]. In high temperatures, such as fire, the  $\text{PbI}_2$  oxidizes into  $\text{PbO}$  and  $\text{PbO}_2$ , both of which are insoluble in water [152, 153].  $\text{PbO}$  powder can be absorbed by the skin and stored in soft tissues. After continual exposure, lead is absorbed into the bone and teeth where it has an elimination half-life of 20–30 years.

The US CDC sets upper limits on acceptable Pb blood level, which in the 1960s was set to 60  $\mu\text{g}/\text{dL}$  and has been reduced over the years to the present value of 5  $\mu\text{g}/\text{dL}$  in adults and 3.5  $\mu\text{g}/\text{dL}$  for children [154, 155]. In adults, even a level of 5  $\mu\text{g}/\text{dL}$  can lead to anemia and increased blood pressure, and exposure to pregnant women could endanger the fetus [156]. Symptoms of lead poisoning generally become noticeable when blood levels reach 40  $\mu\text{g}/\text{dL}$  [157]. Lead is especially dangerous to children because they absorb lead about 4–5x more than adults due to their hand-to-mouth tendencies [158]. Blood levels of 5–10  $\mu\text{g}/\text{dL}$  in children cause an interference with brain development, lowered IQ, decreased hearing, and stunted growth—with the impacts amplified as blood levels rise [156, 158, 159]. The Institute for Health Metrics

and Evaluation (IHME) estimates that as of 2019, 62.5% of the world's intellectual disability without an otherwise obvious source is caused by lead [160].

The US Department of Labor's Occupational Safety and Health Administration (OSHA) enforces safety regulations to provide safe and healthful working conditions for workers [161]. OSHA regulates a wide range of workplace hazards including chemical hazards and safe use of equipment [161]. An estimated 1.6 million workers in the USA are potentially exposed to lead, primarily at construction sites and manufacturing facilities. Employers must take compliance actions if airborne lead levels exceed the "action limit" of  $30 \mu\text{m}/\text{m}^3$ , including medical monitoring, more stringent worksite controls, and the use of respirators, gloves, goggles, and other proper personal protection equipment (PPE) [162]. Additionally, if lead dust or lead-containing materials are present in a workspace, employers must provide proper PPE and require good hygiene practices, such as regular handwashing and showering before leaving the workspace. The National Ambient Air Quality Standards (NAAQS) regulates the ambient air concentration of lead, ozone, carbon monoxide, particulate matter, sulfur dioxide, and nitrogen dioxide. The maximum safe lead level in ambient air is defined as  $0.15 \mu\text{g}/\text{m}^3$  over a 3-month average [163]. Per the US Environmental Protection Agency (EPA), PV modules are categorized as a solid waste and are required to undergo waste characterization prior to disposal. The Comprehensive Environmental Response, Compensation, and Liability Act (CERCLA) of 1980 focuses on the response to a release, or the threatened release, of hazardous substances that may endanger public health or the environment [150, 164]. A site containing high levels of lead in the soil or groundwater meets criteria to be deemed a "superfund site" and qualifies for funding to clean up and rehabilitate the site. CERCLA assesses potential superfund sites for a variety of contaminants, and lead is the most common pollutant. There are currently over 600 recorded superfund sites, 43% of which have lead contamination [164].

Tin (Sn)- and cesium (Cs)-based halide perovskites appear to be less harmful; however, they should not be considered a safe and nontoxic alternative. Tin toxicity is highly dependent on its ionic form. Inorganic tin compounds are expelled from the body quickly but have been found to be harmful in large amounts. Organic tin compounds (organotins), which are commonly used in tin halide perovskites, can cause neurological problems, gastrointestinal symptoms, and respiratory irritation [165, 166]. Tin halide perovskites can degrade to form  $\text{SnO}_2$  and  $\text{SnI}_4$  [167, 168].  $\text{SnI}_4$  is highly reactive with water forming  $\text{SnO}_2$  [167], which can cause respiratory irritation and harm to the aquatic life [169]. Cs-based halide perovskites are attractive due to their high luminescence quantum yield and excellent thermal stability [170]. However, Cs can cause burns and severe irritation to the skin upon contact due to its corrosivity [171]. Inhalation of Cs can result in irritation to the nose, throat, and lungs which may potentially lead to a buildup of fluid in the lungs [172]. In addition, Cs hydroxide also poses a risk to workers in transport and manufacturing due to its intense reactivity with water which could result in burns, inhalation, and ignition of other nearby flammable materials [171].

Events that can result in exposure include accidents, disposal, and module breakage from severe weather or transportation, among others. Accidents during manufacturing include accidental spills, inadequate ventilation, lack of safety protocols,



improper hygiene, and decontamination procedures. Noncompliance with protocols can lead to skin contact, inhalation, or even ingestion of harmful toxins. Storage and transportation of modules present risks. Warehouse storing modules pose fire risk due to the high density of material. Transporting modules present risks of accident, causing module breakage and potential release of hazardous materials that could possess skin contact risk for workers. First Solar, the CdTe thin-film manufacturer, shows that as of 2011 approximately one-third of warranty returns are due to module breakage occurring during the shipping and installation process, corresponding to the return of 0.4% of modules [173].

There are three main exposure pathways of concern: inhalation, ingestion, and skin contact. Inhalation risks stem primarily from fire smoke, but toxic substances in dust or other small particles can be aerosolized from burned or broken modules and cause resultant harm. For some toxic substances, inhalation is the highest-risk exposure pathway due to increased absorption by the body. Common safety practices include maintaining proper ventilation, wearing well-fitting masks with suitable filters, and restricting nonessential workers from accessing specific areas [174]. Ingestion can occur through several routes including contamination of drinking water, children’s play areas, or soil used to grow food. Skin contact is an important exposure pathway for liquid solvents, which can cause skin irritation and burns. Some chemicals can also be absorbed into the body through the skin, putting one at risk for both dermal and internal harm. Proper PPE, particularly gloves, is crucial to prevent exposure through skin contact.

In the case of fires, high temperatures can damage modules and release Pb into the air or into the water used to extinguish the fire. Conings et al. (2019) fire exposure experiments quantified the percentage of lead released from a MHP module during a fire [175]. Analysis of nearby surfaces was assessed to determine the amount of lead carried by the smoke and deposited on surfaces in the vicinity of the fire. Glass encapsulation mostly absorbed the Pb from the MHP layer, and Pb found on nearby surfaces was released from the exposed sections of PV modules where the encapsulation was damaged or destroyed [175].

Leaching can occur when material from the module is exposed to a liquid such as rainwater, water from extinguishing fires, or soil pore water in the case that the modules are disposed of in a landfill. The contaminants dissolve into the water forming ions that leach out of the module through cracks or module edges into groundwater, soil, or be absorbed by nearby plants. The EPA specifies a Toxicity Characteristic Leaching Procedure (TCLP) test (Method 1311) under RCRA for waste characterization [176]. The procedure simulates leaching in a landfill to determine whether hazardous elements will leach from the waste. There are currently TCLP limits on eight heavy metals, some of which may be present in MHP modules. Any material with TCLP analytical results above the regulatory limit is deemed hazardous waste and must be disposed of in facilities permitted to accept such waste.

The pursuit of lead-free or “low-lead” semiconductors as a safer alternative would help mitigate the risk of lead release as they may offer a more environmentally safe route to commercialization. However, current challenges in this area include raising the efficiency and increasing stability of these alternative designs. In the near term, researchers have proposed and demonstrated the use of polymeric



materials in the module packaging that bind to free lead in solution preventing excess leaching and transport [177–180].

## 5.1 Future Work and Challenges

The commercialization of MHP solar modules is a promising technology for achieving the US government's decarbonization goals of 100% carbon-free electricity generation by 2035 [3]. MHP modules are on the cusp of commercialization with several research and manufacturing gaps as final barriers. Reproducible deposition of efficient thin-film MHP solar modules need to be demonstrated at large areas and rapid processing rates. Characterization methods are needed to monitor the quality and performance of products coming off of these high-speed production lines. Validated accelerated test protocols are needed to ensure that modules will survive in the field in a range of climates and conditions. Outdoor performance validation studies in a range of climates are needed to demonstrate that testing protocols are adequate to identify relevant failure and degradation modes. Finally, the safety protocols for workers need to be established, and the environmental risks associated with end of life and/or reuse/recycling need to be considered.

**Acknowledgments** This material is based upon work supported by the US Department of Energy's Office of Energy Efficiency and Renewable Energy (EERE) under the Solar Energy Technologies Office Award Number 38050.

Sandia National Laboratories is a multimission laboratory managed and operated by National Technology & Engineering Solutions of Sandia, LLC, a wholly owned subsidiary of Honeywell International Inc., for the US Department of Energy's National Nuclear Security Administration under contract DE-NA0003525.

This work was authored in part by the National Renewable Energy Laboratory, operated by Alliance for Sustainable Energy, LLC, for the US Department of Energy (DOE) under Contract No. DE-AC36-08GO28308.

The views expressed in the article do not necessarily represent the views of the DOE or the US government. The US government retains, and the publisher, by accepting the article for publication, acknowledges that the US government retains a nonexclusive, paid-up, irrevocable, worldwide license to publish or reproduce the published form of this work, or allow others to do so, for US government purposes.

## References

1. Kojima, A., Teshima, K., Shirai, Y., & Miyasaka, T. (2009). *Organometal halide perovskites as visible-light sensitizers for photovoltaic cells* (Vol. 131, pp. 6050–6051). American Chemical Society.
2. Bellini, E. (2021). *UNIST, EPFL claim 25.6% efficiency world record for perovskite solar cell*.
3. Siegler, T. D. et al. (2022). The path to perovskite commercialization: A perspective from the United States solar energy technologies office. *ACS Energy Letters*, 1728–1734. <https://doi.org/10.1021/acsenerylett.2c00698>.

4. Smith, B. L., Woodhouse, M., Horowitz, K. A. W., Silverman, T. J., Zuboy, J., & Margolis, R. M. (2021). *Photovoltaic (PV) Module Technologies\_2020 Benchmark costs and technology evolution framework results*. NREL.
5. Wilson, G. M., et al. (2020). The 2020 photovoltaic technologies roadmap. *Journal of Physics D: Applied Physics*, 53. <https://doi.org/10.1088/1361-6463/ab9c6a>
6. Pérez-Gutiérrez, E., et al. (2017). Organic solar cells all made by blade and slot–die coating techniques. *Solar Energy*, 146, 79–84. <https://doi.org/10.1016/j.solener.2017.02.004>
7. Yang, Z., Zhang, W., Wu, S., Zhu, H., Liu, Z., Lui, Z., Jiang, Z., Chen, R., & Zhou, J. (2021). Slot-die coating large-area formamidinium-cesium perovskite film for efficient and stable parallel solar module.
8. Rong, Y., et al. (2018). Toward industrial-scale production of perovskite solar cells: Screen printing, slot-die coating, and emerging techniques. *Journal of Physical Chemistry Letters*, 9, 2707–2713. <https://doi.org/10.1021/acs.jpcllett.8b00912>
9. Liu, C., Cheng, Y. B., & Ge, Z. (2020). Understanding of perovskite crystal growth and film formation in scalable deposition processes. *Chemical Society Reviews*, 49, 1653–1687. <https://doi.org/10.1039/c9cs00711c>
10. Bishop, J. E., Smith, J. A., & Lidzey, D. G. (2020). Development of spray-coated perovskite solar cells. *ACS Applied Materials & Interfaces*, 12, 48237–48245. <https://doi.org/10.1021/acsaami.0c14540>
11. Lee, D. S., et al. (2022). Fully scalable and stable CsPbI<sub>2</sub>Br solar cells realized by an all-spray-coating process. *ACS Applied Materials & Interfaces*, 14, 7926–7935. <https://doi.org/10.1021/acsaami.1c21644>
12. Parida, B. et al. (2022). Recent developments in upscalable printing techniques for perovskite solar cells. *Advanced Science (Weinh)*, e2200308. <https://doi.org/10.1002/advs.202200308>.
13. Howard, I. A., et al. (2019). Coated and printed perovskites for photovoltaic applications. *Advanced Materials*, 31, e1806702. <https://doi.org/10.1002/adma.201806702>
14. Castro-Hermosa, S., et al. (2020). Efficient fully blade-coated perovskite solar cells in air with nanometer-thick bathocuproine buffer layer. *Nano Research*, 14, 1034–1042. <https://doi.org/10.1007/s12274-020-3147-4>
15. Liang, Q., et al. (2022). Manipulating crystallization kinetics in high-performance blade-coated perovskite solar cells via cosolvent-assisted phase transition. *Advanced Materials*, e2200276. <https://doi.org/10.1002/adma.202200276>.
16. Razza, S., et al. (2015). Perovskite solar cells and large area modules (100 cm<sup>2</sup>) based on an air flow-assisted PbI<sub>2</sub> blade coating deposition process. *Journal of Power Sources*, 277, 286–291. <https://doi.org/10.1016/j.jpowsour.2014.12.008>
17. Ouyang, Z., Yang, M., Whitaker, J. B., Li, D., & van Hest, M. F. A. M. (2020). Toward scalable perovskite solar modules using blade coating and rapid thermal processing. *ACS Applied Energy Materials*, 3, 3714–3720. <https://doi.org/10.1021/acsaem.0c00180>
18. de Oliveira, M. C. C., Diniz Cardoso, A. S. A., Viana, M. M., & Lins, V. D. F. C. (2018). The causes and effects of degradation of encapsulant ethylene vinyl acetate copolymer (EVA) in crystalline silicon photovoltaic modules: A review. *Renewable and Sustainable Energy Reviews*, 81, 2299–2317. <https://doi.org/10.1016/j.rser.2017.06.039>
19. Li, J., et al. (2021). Encapsulation of perovskite solar cells for enhanced stability: Structures, materials and characterization. *Journal of Power Sources*, 485. <https://doi.org/10.1016/j.jpowsour.2020.229313>
20. Wang, Y., et al. (2022). Encapsulation and stability testing of perovskite solar cells for real life applications. *ACS Materials Au*, 2, 215–236. <https://doi.org/10.1021/acsmaterialsau.1c00045>
21. Liu, Z., et al. (2020). A holistic approach to interface stabilization for efficient perovskite solar modules with over 2,000-hour operational stability. *Nature Energy*, 5, 596–604. <https://doi.org/10.1038/s41560-020-0653-2>
22. Tong, G., et al. (2021). Scalable fabrication of >90 cm<sup>2</sup> perovskite solar modules with >1000 h operational stability based on the intermediate phase strategy. *Advanced Energy Materials*, 11. <https://doi.org/10.1002/aenm.202003712>

23. Sha, Y., et al. (2020). A scalable integrated dopant-free heterostructure to stabilize perovskite solar cell modules. *Advanced Energy Materials*, 11. <https://doi.org/10.1002/aenm.202003301>
24. Jiang, Y., et al. (2018). Combination of hybrid CVD and cation exchange for upscaling Cs-substituted mixed cation perovskite solar cells with high efficiency and stability. *Advanced Functional Materials*, 28. <https://doi.org/10.1002/adfm.201703835>
25. Jiang, Y., et al. (2019). Negligible-Pb-waste and upscalable perovskite deposition technology for high-operational-stability perovskite solar modules. *Advanced Energy Materials*, 9. <https://doi.org/10.1002/aenm.201803047>
26. Bu, T., et al. (2019). Dynamic antisolvent engineering for spin coating of  $10 \times 10$  cm<sup>2</sup> perovskite solar module approaching 18%. *Solar RRL*, 4. <https://doi.org/10.1002/solr.201900263>
27. Dai, X., et al. (2019). Scalable fabrication of efficient perovskite solar modules on flexible glass substrates. *Advanced Energy Materials*, 10. <https://doi.org/10.1002/aenm.201903108>
28. Chiang, C.-H., Nazeeruddin, M. K., Grätzel, M., & Wu, C.-G. (2017). The synergistic effect of H<sub>2</sub>O and DMF towards stable and 20% efficiency inverted perovskite solar cells. *Energy & Environmental Science*, 10, 808–817. <https://doi.org/10.1039/c6ee03586h>
29. Hu, C., et al. (2021). Discovery of a new intermediate enables one-step deposition of high-quality perovskite films via solvent engineering. *Solar RRL*, 5. <https://doi.org/10.1002/solr.202000712>
30. Im, J.-H., Kim, H.-S., & Park, N.-G. (2014). Morphology-photovoltaic property correlation in perovskite solar cells: One-step versus two-step deposition of CH<sub>3</sub>NH<sub>3</sub>PbI<sub>3</sub>. *APL Materials*, 2. <https://doi.org/10.1063/1.4891275>
31. Liu, Z., et al. (2021). Scalable one-step heating up synthesis of Cu<sub>2</sub>ZnSnS<sub>4</sub> nanocrystals hole conducting materials for carbon electrode based perovskite solar cells. *Solar Energy*, 224, 51–57. <https://doi.org/10.1016/j.solener.2021.05.089>
32. Christians, J. A., et al. (2018). Stability at scale: Challenges of module interconnects for perovskite photovoltaics. *ACS Energy Letters*, 3, 2502–2503. <https://doi.org/10.1021/acsenerylett.8b01498>
33. Yang, M., et al. (2017). Perovskite ink with wide processing window for scalable high-efficiency solar cells. *Nature Energy*, 2. <https://doi.org/10.1038/nenergy.2017.38>
34. Nair, S., Patel, S. B., & Gohel, J. V. (2020). Recent trends in efficiency-stability improvement in perovskite solar cells. *Materials Today Energy*, 17. <https://doi.org/10.1016/j.mtener.2020.100449>
35. Qiu, L., et al. (2019). Hybrid chemical vapor deposition enables scalable and stable Cs-FA mixed cation perovskite solar modules with a designated area of 91.8 cm<sup>2</sup> approaching 10% efficiency. *Journal of Materials Chemistry A*, 7, 6920–6929. <https://doi.org/10.1039/c9ta00239a>
36. Leyden, M. R., Jiang, Y., & Qi, Y. (2016). Chemical vapor deposition grown formamidinium perovskite solar modules with high steady state power and thermal stability. *Journal of Materials Chemistry A*, 4, 13125–13132. <https://doi.org/10.1039/c6ta04267h>
37. Li, J., et al. (2020). Highly efficient thermally co-evaporated perovskite solar cells and mini-modules. *Joule*, 4, 1035–1053. <https://doi.org/10.1016/j.joule.2020.03.005>
38. Compaan, A. D., Gupta, A., Lee, S., Wang, S., & Drayton, J. (2004). High efficiency, magnetron sputtered CdS/CdTe solar cells. *Solar Energy*, 77, 815–822. <https://doi.org/10.1016/j.solener.2004.06.013>
39. Ramanujam, J., et al. (2020). Flexible CIGS, CdTe and a-Si:H based thin film solar cells: A review. *Progress in Materials Science*, 110. <https://doi.org/10.1016/j.pmatsci.2019.100619>
40. Han, G. S., et al. (2019). Spin-coating process for 10 cm × 10 cm perovskite solar modules enabled by self-assembly of SnO<sub>2</sub> nanocolloids. *ACS Energy Letters*, 4, 1845–1851. <https://doi.org/10.1021/acsenerylett.9b00953>
41. Park, N.-G., & Zhu, K. (2020). Scalable fabrication and coating methods for perovskite solar cells and solar modules. *Nature Reviews Materials*, 5, 333–350. <https://doi.org/10.1038/s41578-019-0176-2>

42. Cheng, R., et al. (2019). An air knife-assisted recrystallization method for ambient-process planar perovskite solar cells and its dim-light harvesting. *Small*, *15*, e1804465. <https://doi.org/10.1002/sml.201804465>
43. Zhang, X., Yang, W., Qi, J., & Hu, Y. (2020). Preparing ambient-processed perovskite solar cells with better electronic properties via preheating assisted one-step deposition method. *Nanoscale Research Letters*, *15*, 178. <https://doi.org/10.1186/s11671-020-03407-9>
44. Li, P., Omer Mohamed, M. I., Xu, C., Wang, X., & Tang, X. (2020). Electrical property modified hole transport layer (PEDOT:PSS) enhance the efficiency of perovskite solar cells: Hybrid co-solvent post-treatment. *Organic Electronics*, *78*. <https://doi.org/10.1016/j.orgel.2019.105582>
45. Li, C.-Y., et al. (2021). Anti-solvent mixture-mediated reduction of photocurrent hysteresis in high-impurity perovskite precursor based MAPbI<sub>3</sub> solar cells. *Solar Energy*, *214*, 86–92. <https://doi.org/10.1016/j.solener.2020.11.062>
46. Lee, D.-K., Lim, K.-S., Lee, J.-W., & Park, N.-G. (2021). Scalable perovskite coating via anti-solvent-free Lewis acid–base adduct engineering for efficient perovskite solar modules. *Journal of Materials Chemistry A*, *9*, 3018–3028. <https://doi.org/10.1039/d0ta10366g>
47. Zhang, F., & Zhu, K. (2019). Additive engineering for efficient and stable perovskite solar cells. *Advanced Energy Materials*, *10*. <https://doi.org/10.1002/aenm.201902579>
48. Liu, Y., et al. (2021). Ionic additive engineering for stable planar perovskite solar cells with efficiency >22%. *Chemical Engineering Journal*, *426*. <https://doi.org/10.1016/j.cej.2021.130841>
49. Li, Y., Dailey, M., Lohr, P. J., & Printz, A. D. (2021). Performance and stability improvements in metal halide perovskite with intralayer incorporation of organic additives. *Journal of Materials Chemistry A*, *9*, 16281–16338. <https://doi.org/10.1039/d1ta05252g>
50. Conings, B., et al. (2015). The impact of precursor water content on solution-processed organometal halide perovskite films and solar cells. *Journal of Materials Chemistry A*, *3*, 19123–19128. <https://doi.org/10.1039/c5ta06199g>
51. Sakai, N., et al. (2017). Controlling nucleation and growth of metal halide perovskite thin films for high-efficiency perovskite solar cells. *Small*, *13*. <https://doi.org/10.1002/sml.201602808>
52. Cheng, Y., Peng, Y., Jen, A. K. Y., & Yip, H.-L. (2021). Development and challenges of metal halide perovskite solar modules. *Solar RRL*, <https://doi.org/10.1002/solr.202100545>.
53. Zhong, J. X., Wu, W. Q., Ding, L., & Kuang, D. B. (2020). Blade-coating perovskite films with diverse compositions for efficient photovoltaics. *Energy & Environmental Materials*, *4*, 277–283. <https://doi.org/10.1002/eem2.12118>
54. Gao, L.-L., Li, C.-X., Li, C.-J., & Yang, G.-J. (2017). Large-area high-efficiency perovskite solar cells based on perovskite films dried by the multi-flow air knife method in air. *Journal of Materials Chemistry A*, *5*, 1548–1557. <https://doi.org/10.1039/c6ta09565h>
55. Abdelsamie, M., et al. (2020). Impact of Processing on Structural and Compositional Evolution in Mixed Metal Halide Perovskites during Film Formation. *Advanced Functional Materials*, *30*. <https://doi.org/10.1002/adfm.202001752>
56. Zhang, H., et al. (2022). A universal co-solvent dilution strategy enables facile and cost-effective fabrication of perovskite photovoltaics. *Nature Communications*, *13*, 89. <https://doi.org/10.1038/s41467-021-27740-4>
57. Liu, R., et al. (2020). The synergistic effect of co-solvent engineering and thermal engineering towards phase control two-dimensional perovskite solar cells. *Solar Energy*, *209*, 446–453. <https://doi.org/10.1016/j.solener.2020.09.006>
58. Ha, S. T., Su, R., Xing, J., Zhang, Q., & Xiong, Q. (2017). Metal halide perovskite nanomaterials: Synthesis and applications. *Chemical Science*, *8*, 2522–2536. <https://doi.org/10.1039/c6sc04474c>
59. Sun, J., Li, F., Yuan, J., & Ma, W. (2021). Advances in metal halide perovskite film preparation: The role of anti-solvent treatment. *Small Methods*, *5*, e2100046. <https://doi.org/10.1002/smt.202100046>

60. Li, M., et al. (2017). Enhanced efficiency and stability of perovskite solar cells via anti-solvent treatment in two-step deposition method. *ACS Applied Materials & Interfaces*, 9, 7224–7231. <https://doi.org/10.1021/acsami.7b01136>
61. Lee, D. S., et al. (2019). Grain quality engineering for organic metal halide perovskites using mixed antisolvent spraying treatment. *Solar RRL*, 4. <https://doi.org/10.1002/solr.201900397>
62. Moot, T., et al. (2020). CsI-antisolvent adduct formation in all-inorganic metal halide perovskites. *Advanced Energy Materials*, 10. <https://doi.org/10.1002/aenm.201903365>
63. Lee, J. W., Kim, H. S., & Park, N. G. (2016). Lewis acid-base adduct approach for high efficiency perovskite solar cells. *Accounts of Chemical Research*, 49, 311–319. <https://doi.org/10.1021/acs.accounts.5b00440>
64. Wang, S., et al. (2020). Lewis acid/base approach for efficacious defect passivation in perovskite solar cells. *Journal of Materials Chemistry A*, 8, 12201–12225. <https://doi.org/10.1039/d0ta03957h>
65. Jia, Q., et al. (2020). Large-grained all-inorganic bismuth-based perovskites with narrow band gap via lewis acid-base adduct approach. *ACS Applied Materials & Interfaces*, 12, 43876–43884. <https://doi.org/10.1021/acsami.0c14512>
66. Abbas, M., et al. (2020). A critical review on crystal growth techniques for scalable deposition of photovoltaic perovskite thin films. *Materials (Basel)*, 13. <https://doi.org/10.3390/ma13214851>
67. Reddy, S. S., et al. (2019). Lewis acid-base adduct-type organic hole transport material for high performance and air-stable perovskite solar cells. *Nano Energy*, 58, 284–292. <https://doi.org/10.1016/j.nanoen.2019.01.041>
68. Heo, Y. J., et al. (2021). Enhancing performance and stability of tin halide perovskite light emitting diodes via coordination engineering of lewis acid–base adducts. *Advanced Functional Materials*, 31. <https://doi.org/10.1002/adfm.202106974>
69. Sun, H., et al. (2021). Strategies and methods for fabricating high quality metal halide perovskite thin films for solar cells. *Journal of Energy Chemistry*, 60, 300–333. <https://doi.org/10.1016/j.jechem.2021.01.001>
70. Liu, C., et al. (2020). Tailoring C60 for efficient inorganic CsPbI<sub>2</sub> Br perovskite solar cells and modules. *Advanced Materials*, 32, e1907361. <https://doi.org/10.1002/adma.201907361>
71. Abdelsamie, M., et al. (2021). Mechanism of additive-assisted room-temperature processing of metal halide perovskite thin films. *ACS Applied Materials & Interfaces*, 13, 13212–13225. <https://doi.org/10.1021/acsami.0c22630>
72. Liu, Z., Ono, L. K., & Qi, Y. (2020). Additives in metal halide perovskite films and their applications in solar cells. *Journal of Energy Chemistry*, 46, 215–228. <https://doi.org/10.1016/j.jechem.2019.11.008>
73. Ling, J., et al. (2021). A perspective on the commercial viability of perovskite solar cells. *Solar RRL*, 5. <https://doi.org/10.1002/solr.202100401>
74. Vesce, L., et al. (2021). Ambient air blade-coating fabrication of stable triple-cation perovskite solar modules by green solvent quenching. *Solar RRL*, 5. <https://doi.org/10.1002/solr.202100073>
75. Tian, S., et al. (2019). A facile green solvent engineering for up-scaling perovskite solar cell modules. *Solar Energy*, 183, 386–391. <https://doi.org/10.1016/j.solener.2019.03.038>
76. Zhang, M., Xin, D., Zheng, X., Chen, Q., & Zhang, W.-H. (2020). Toward Greener solution processing of perovskite solar cells. *ACS Sustainable Chemistry & Engineering*, 8, 13126–13138. <https://doi.org/10.1021/acssuschemeng.0c04289>
77. Hoang, M. T., et al. (2021). Towards the environmentally friendly solution processing of metal halide perovskite technology. *Green Chemistry*, 23, 5302–5336. <https://doi.org/10.1039/d1gc01756j>
78. Cui, Y., Wang, S., Ding, L., & Hao, F. (2020). Green-solvent-processable perovskite solar cells. *Advanced Energy and Sustainability Research*, 2. <https://doi.org/10.1002/aesr.202000047>

79. Ahmed, D. S., Mohammed, B. K., & Mohammed, M. K. A. (2021). Long-term stable and hysteresis-free planar perovskite solar cells using green antisolvent strategy. *Journal of Materials Science*, 56, 15205–15214. <https://doi.org/10.1007/s10853-021-06200-w>
80. Bu, T., et al. (2017). Synergic interface optimization with green solvent engineering in mixed perovskite solar cells. *Advanced Energy Materials*, 7. <https://doi.org/10.1002/aenm.201700576>
81. Worsley, C., et al. (2021).  $\gamma$ -Valerolactone: A nontoxic green solvent for highly stable printed mesoporous perovskite solar cells. *Energy Technology*, 9. <https://doi.org/10.1002/ente.202100312>
82. Worsley, C., et al. (2022). Green solvent engineering for enhanced performance and reproducibility in printed carbon-based mesoscopic perovskite solar cells and modules. *Materials Advances*, 3, 1125–1138. <https://doi.org/10.1039/d1ma00975c>
83. Rakocevic, L., et al. (2017). Interconnection optimization for highly efficient perovskite modules. *IEEE Journal of Photovoltaics*, 7, 404–408. <https://doi.org/10.1109/jphotov.2016.2626144>
84. Yang, M., et al. (2018). Highly efficient perovskite solar modules by scalable fabrication and interconnection optimization. *ACS Energy Letters*, 3, 322–328. <https://doi.org/10.1021/acsenerylett.7b01221>
85. Bailie, C., Eberspacher, C., Gehan, E., Bramante, R., & Hest, M. (2019). In *IEEE 46th photovoltaic specialists conference*, 1–5.
86. Kim, D. H., Whitaker, J. B., Li, Z., van Hest, M. F. A. M., & Zhu, K. (2018). Outlook and challenges of perovskite solar cells toward terawatt-scale photovoltaic module technology. *Joule*, 2, 1437–1451. <https://doi.org/10.1016/j.joule.2018.05.011>
87. Razza, S., Pescetelli, S., Agresti, A., & Di Carlo, A. (2021). Laser processing optimization for large-area perovskite solar modules. *Energies*, 14. <https://doi.org/10.3390/en14041069>
88. Rong, Y., et al. (2018). Challenges for commercializing perovskite solar cells. *Science*, 361. <https://doi.org/10.1126/science.aat8235>
89. Di Giacomo, F., et al. (2020). Upscaling Inverted perovskite solar cells: Optimization of laser scribing for highly efficient mini-modules. *Micromachines (Basel)*, 11. <https://doi.org/10.3390/mi11121127>
90. Klaus Ellmer, A. K. B. R. (2007). *Transparent conductive zinc oxide* (Vol. 104). Springer.
91. Walter, A., et al. (2018). Closing the cell-to-module efficiency gap: A fully laser scribed perovskite minimodule with 16% steady-state aperture area efficiency. *IEEE Journal of Photovoltaics*, 8, 151–155. <https://doi.org/10.1109/jphotov.2017.2765082>
92. Tamai, H., & Sato, T. (2020). *Japan's NEDO and panasonic achieve the world's highest conversion efficiency of 16.09% for largest-area perovskite solar cell module*. <https://www.businesswire.com/news/home/20200206006046/en/Japan%E2%80%99s-NEDO-and-Panasonic-Achieve-the-World%E2%80%99s-Highest-Conversion-Efficiency-of-16.09-for-Largest-area-Perovskite-Solar-Cell-Module>
93. Li, H., et al. (2020). Recent progress towards roll-to-roll manufacturing of perovskite solar cells using slot-die processing. *Flexible and Printed Electronics*, 5. <https://doi.org/10.1088/2058-8585/ab639e>
94. Angmo, D., et al. (2021). A lab-to-fab study toward roll-to-roll fabrication of reproducible perovskite solar cells under ambient room conditions. *Cell Reports Physical Science*, 2. <https://doi.org/10.1016/j.xcrp.2020.100293>
95. Martin, B., Amos, D., Brehob, E., van Hest, M. F. A. M., & Druffel, T. (2021). Techno-economic analysis of roll-to-roll production of perovskite modules using radiation thermal processes. *Applied Energy*. <https://doi.org/10.1016/j.apenergy.2021.118200>
96. Zhong, Z. W., Shan, X. C., & Wong, S. J. (2011). Roll-to-roll large-format slot die coating of photosensitive resin for UV embossing. *Microsystem Technologies*, 17, 1703–1711. <https://doi.org/10.1007/s00542-011-1344-5>
97. Moon, S.-J., et al. (2015). Laser-scribing patterning for the production of organometallic halide perovskite solar modules. *IEEE Journal of Photovoltaics*, 5, 1087–1092. <https://doi.org/10.1109/jphotov.2015.2416913>



98. Meroni, S. M. P., et al. (2020). Scribing method for carbon perovskite solar modules. *Energies*, 13. <https://doi.org/10.3390/en13071589>
99. Markauskas, E., Gečys, P., Repins, I., Beall, C., & Račiukaitis, G. (2017). Laser lift-off scribing of the CZTSe thin-film solar cells at different pulse durations. *Solar Energy*, 150, 246–254. <https://doi.org/10.1016/j.solener.2017.01.074>
100. Castriotta, L. A., et al. (2022). Reducing losses in perovskite large area solar technology: Laser design optimization for highly efficient modules and minipanel. *Advanced Energy Materials*, <https://doi.org/10.1002/aenm.202103420>.
101. Taheri, B., et al. (2021). Laser-scribing optimization for sprayed SnO<sub>2</sub>-based perovskite solar modules on flexible plastic substrates. *ACS Applied Energy Materials*, 4, 4507–4518. <https://doi.org/10.1021/acs.aem.1c00140>
102. Lee, D.-K., & Park, N.-G. (2021). Materials and methods for high-efficiency perovskite solar modules. *Solar RRL*, <https://doi.org/10.1002/solr.202100455>.
103. Jung, E. H., et al. (2019). Efficient, stable and scalable perovskite solar cells using poly(3-hexylthiophene). *Nature*, 567, 511–515. <https://doi.org/10.1038/s41586-019-1036-3>
104. Deng, Y., et al. (2018). Surfactant-controlled ink drying enables high-speed deposition of perovskite films for efficient photovoltaic modules. *Nature Energy*, 3, 560–566. <https://doi.org/10.1038/s41560-018-0153-9>
105. International Standard IEC 60904-1 {ed2.0}. (2006–09).
106. Silverman, T., Jahn, U., Apolloni, M., Louwen, A., Schweiger, M., Bellurado, G., Wagner, J., Tetzlaff, A., Ingenhoven, P., & Moser, D. (2014). Characterisation of performance of thin film PV technologies. (International Energy Agency Project: IEA PVPS Task 13).
107. Silverman, T. J., Jahn, U., Friesen, G., Pravettoni, M., Apolloni, M., Louwen, A., van Sark, W. G. J. H. M., Schweiger, M., Bellurado, G., Wagner, J., Tetzlaff, A., Ingenhoven, P., & Moser, D. (2020). In *IEA International Energy Agency* (SFOE NREL, 2020).
108. Silverman, T., Jahn, U., Friesen, G., Pravettoni, M., Apolloni, M., Louwen, A., Schweiger, M., Bellurado, G., Wagner, J., Tetzlaff, A., & Moser, I. D. (2014). IEA-PVPS\_T13-02\_2014\_Characterization\_ThinFilm\_Modules.
109. Bardizza, G., Müllejans, H., Pavanello, D., & Dunlop, E. D. (2021). Metastability in performance measurements of perovskite PV devices: A systematic approach. *Journal of Physics: Energy*, 3. <https://doi.org/10.1088/2515-7655/abd678>
110. Fu, Y. (2022). Stabilization of metastable halide perovskite lattices in the 2D limit. *Advanced Materials*, 34, e2108556. <https://doi.org/10.1002/adma.202108556>
111. Fell, C. J. (2019). Standardising current–voltage measurements for metastable solar cells. *Journal of Physics: Energy*, 2. <https://doi.org/10.1088/2515-7655/ab55cc>
112. Silverman, T. J., M. G. D., Marion, B., Krutz, S. R. (2014). In *2014 IEEE 40th Photovoltaic Specialist Conference (PVSC)*.
113. Yan, X., et al. (2022). Ion migration in hybrid perovskites: Classification, identification, and manipulation. *Nano Today*, 44. <https://doi.org/10.1016/j.nantod.2022.101503>
114. Deceglie, M. G., et al. (2015). Validated method for repeatable power measurement of cigs modules exhibiting light-induced metastabilities. *IEEE Journal of Photovoltaics*, 5, 607–612. <https://doi.org/10.1109/jphotov.2014.2376056>
115. Zhang, S., et al. (2022). Improved performance and stability of perovskite solar modules by interface modulating with graphene oxide crosslinked CsPbBr<sub>3</sub> quantum dots. *Energy & Environmental Science*, 15, 244–253. <https://doi.org/10.1039/d1ee01778k>
116. Kim, H. S., et al. (2015). Control of I–V hysteresis in CH<sub>3</sub>NH<sub>3</sub>PbI<sub>3</sub> perovskite solar cell. *Journal of Physical Chemistry Letters*, 6, 4633–4639. <https://doi.org/10.1021/acs.jpcllett.5b02273>
117. Yan, X., W. F., Cheng, F., Sun, H., Xu, C., Wang, L., Kang, Z., Zhang, Y. (2022). Ion migration in perovskite solar cells. *Science Direct*.
118. Xiaoxue Ren, L. Z., Yongbo Yuan, Liming Ding. (2021). Ion migration in perovskite solar cells. *Journal of Semiconductors*. <https://doi.org/10.1088/1674-4926/42/1/010201>.



119. Zhu, W., et al. (2022). Ion migration in organic-inorganic hybrid perovskite solar cells: current understanding and perspectives. *Small*, *18*, e2105783. <https://doi.org/10.1002/sml.202105783>
120. Elumalai, N. K., & Uddin, A. (2016). Hysteresis in organic-inorganic hybrid perovskite solar cells. *Solar Energy Materials and Solar Cells*, *157*, 476–509. <https://doi.org/10.1016/j.solmat.2016.06.025>
121. Martiradonna, L. (2018). Riddles in perovskite research. *Nature Materials*, *17*, 377. <https://doi.org/10.1038/s41563-018-0072-y>
122. Doumon, N. Y. (2019). The degradation of organic solar cells: From chemistry to device physics through materials. <https://doi.org/10.33612/diss.98539626>.
123. Wohlgemuth, J. (2020). *Photovoltaic Module Reliability*.
124. Reese, M. O., et al. (2011). Consensus stability testing protocols for organic photovoltaic materials and devices. *Solar Energy Materials and Solar Cells*, *95*, 1253–1267. <https://doi.org/10.1016/j.solmat.2011.01.036>
125. Asuo, I. M., et al. (2020). Ambient condition-processing strategy for improved air-stability and efficiency in mixed-cation perovskite solar cells. *Materials Advances*, *1*, 1866–1876. <https://doi.org/10.1039/d0ma00528b>
126. Khenkin, M. V., et al. (2020). Consensus statement for stability assessment and reporting for perovskite photovoltaics based on ISOS procedures. *Nature Energy*, *5*, 35–49. <https://doi.org/10.1038/s41560-019-0529-5>
127. Doumon, N. Y., Yang, L., & Rosei, F. (2022). Ternary organic solar cells: A review of the role of the third element. *Nano Energy*, *94*. <https://doi.org/10.1016/j.nanoen.2021.106915>
128. Schelhas, L. T., et al. (2019). Insights into operational stability and processing of halide perovskite active layers. *Energy & Environmental Science*, *12*, 1341–1348. <https://doi.org/10.1039/c8ee03051k>
129. Bryant, D., et al. (2016). Light and oxygen induced degradation limits the operational stability of methylammonium lead triiodide perovskite solar cells. *Energy & Environmental Science*, *9*, 1655–1660. <https://doi.org/10.1039/c6ee00409a>
130. Mundt, L. E., et al. (2021). Mixing matters: Nanoscale heterogeneity and stability in metal halide perovskite solar cells. *ACS Energy Letters*, *7*, 471–480. <https://doi.org/10.1021/acsenergylett.1c02338>
131. Song, Z., et al. (2015). Impact of processing temperature and composition on the formation of methylammonium lead iodide perovskites. *Chemistry of Materials*, *27*, 4612–4619. <https://doi.org/10.1021/acs.chemmater.5b01017>
132. Luchkin, S. Y., et al. (2017). Reversible and irreversible electric field induced morphological and interfacial transformations of hybrid lead iodide perovskites. *ACS Applied Materials & Interfaces*, *9*, 33478–33483. <https://doi.org/10.1021/acsmi.7b01960>
133. Wang, J., et al. (2021). Tuning an electrode work function using organometallic complexes in inverted perovskite solar cells. *Journal of the American Chemical Society*, *143*, 7759–7768. <https://doi.org/10.1021/jacs.1c02118>
134. Schulz, P., Cahen, D., & Kahn, A. (2019). *Halide perovskites: Is it all about the interfaces?* (Vol. 119, pp. 3349–3417). American Chemical Society.
135. Dunfield, S. P., et al. (2020). From defects to degradation: A mechanistic understanding of degradation in perovskite solar cell devices and modules. *Advanced Energy Materials*, *10*. <https://doi.org/10.1002/aenm.201904054>
136. Motti, S. G., et al. (2019). Controlling competing photochemical reactions stabilizes perovskite solar cells. *Nature Photonics*, *13*, 532–539. <https://doi.org/10.1038/s41566-019-0435-1>
137. Akriti et al. Layer-by-layer anionic diffusion in two-dimensional halide perovskite vertical heterostructures. *Nature Nanotechnology* *16*, 584–591, doi:<https://doi.org/10.1038/s41565-021-00848-w> (2021).
138. Cho, J., Mathew, P. S., DuBose, J. T., & Kamat, P. V. (2021). Photoinduced halide segregation in ruddlesden-popper 2D mixed halide perovskite films. *Advanced Materials*, *33*, e2105585. <https://doi.org/10.1002/adma.202105585>

139. Ding, Y., et al. (2022). Single-crystalline TiO<sub>2</sub> nanoparticles for stable and efficient perovskite modules. *Nature Nanotechnology*, 17, 598–605. <https://doi.org/10.1038/s41565-022-01108-1>
140. Rehman, A. U., et al. (2021). Electrode metallization for scaled perovskite/silicon tandem solar cells: Challenges and opportunities. *Progress in Photovoltaics: Research and Applications*. <https://doi.org/10.1002/pip.3499>
141. S. Kurtz, J. Wohlgemuth, M. Kempe, N. Bosco, P. Hacke, D. Jordan, D. C. Miller, T. J. Silverman. (2013). *Photovoltaic module qualification plus testing*.
142. Smokler, M. I., Otth, D. H., & Ross, R. G. Jr. (1985). In *Proceedings of the 18th IEEE photovoltaic specialists conference* (Las Vegas, Nevada).
143. Doyle, T., Desharnais, R., & Lorico, T. E. (2020). *2020 PVEL PV module reliability scorecard*.
144. Owen-Bellini, M., et al. (2020). Advancing reliability assessments of photovoltaic modules and materials using combined-accelerated stress testing. *Progress in Photovoltaics: Research and Applications*, 29, 64–82. <https://doi.org/10.1002/pip.3342>
145. Jeong, S.-H., et al. (2020). Characterizing the efficiency of perovskite solar cells and light-emitting diodes. *Joule*, 4, 1206–1235. <https://doi.org/10.1016/j.joule.2020.04.007>
146. Dunbar, R. B., et al. (2017). How reliable are efficiency measurements of perovskite solar cells? The first inter-comparison, between two accredited and eight non-accredited laboratories. *Journal of Materials Chemistry A*, 5, 22542–22558. <https://doi.org/10.1039/c7ta05609e>
147. *DuraMat Durable Module Materials Consortium*.
148. Torrence, C. E., Libby, C. S., Nie, W., Stein, J. S. (2023) Environmental and health risks of perovskite solar modules: Case for better test standards and risk mitigation solutions. *iScience*, 26(1), 105807. <https://doi.org/10.1016/j.isci.2022.105807>
149. Angelidis, T. N., & Kydros, K. A. (1995). Selective gold dissolution from a roasted auriferous pyrite-arsenopyrite concentrate. *Hydrometallurgy*, 37, 75–88.
150. Clever, H. L., & Johnston, F. J. (1980). The solubility of some sparingly soluble lead salts: An evaluation of the solubility in water and aqueous electrolyte solution. *Journal of Physical and Chemical Reference Data*, 9, 751–784. <https://doi.org/10.1063/1.555628>
151. Lichy, D. M. (1903). The solubility of the chloride, the bromide, and the iodide of lead, in water, at temperatures from 0° upward. *ACS*, 25, 469–474. <https://doi.org/10.1021/ja02007a002>
152. New Jersey Department of Health. Hazardous Substance Fact Sheet Cesium Hydroxide. (2007).
153. Garcia, G., et al. (2018). Influence of chromium hyperdoping on the electronic structure of CH<sub>3</sub>NH<sub>3</sub>PbI<sub>3</sub> perovskite: A first-principles insight. *Scientific Reports*, 8, 2511. <https://doi.org/10.1038/s41598-018-20851-x>
154. Galvao, J., et al. (2014). Unexpected low-dose toxicity of the universal solvent DMSO. *The FASEB Journal*, 28, 1317–1330. <https://doi.org/10.1096/fj.13-235440>
155. Agency for Toxic Substances and Disease Registry (ATSDR) What are the physiologic effects of chromium exposure? (Center for Disease Control, Agency for Toxic Substances and Disease Registry (ATSDR) Environmental Health and Medicine Education, 2013).
156. Lee, K. P., Chromey, N. C., Culik, R., Barnes, J. R., & Schneider, P. W. (1987). Toxicity of N-methyl-2-pyrrolidone (NMP) Teratogenic, subchronic, and two-year inhalation studies. *PubMed*, 9. [https://doi.org/10.1016/0272-0590\(87\)90045-5](https://doi.org/10.1016/0272-0590(87)90045-5)
157. Scailteur, V., & Lauwerys, R. R. (1987). Dimethylformamide (DMF) hepatotoxicity. *Toxicology*, 43, 231–238. [https://doi.org/10.1016/0300-483x\(87\)90082-5](https://doi.org/10.1016/0300-483x(87)90082-5)
158. Foxall, K. (Ed.). (2007). *Chemical and Environmental hazards UK HPA Centre for Radiation*.
159. Sinha, P., Balas, R., Krueger, L., & Wade, A. (2012). Fate and transport evaluation of potential leaching risks from cadmium telluride photovoltaics. *Environmental Toxicology and Chemistry*, 31, 1670–1675. <https://doi.org/10.1002/etc.1865>
160. Labor, U. S. D. o. *Occupational safety and health administration* <<https://www.osha.gov/solvents>>.

161. Li, J., et al. (2020). Biological impact of lead from halide perovskites reveals the risk of introducing a safe threshold. *Nature Communications*, *11*, 310. <https://doi.org/10.1038/s41467-019-13910-y>
162. Natasha, et al. (2020). Risk assessment and biophysiochemical responses of spinach to foliar application of lead oxide nanoparticles: A multivariate analysis. *Chemosphere*, *245*, 125605. <https://doi.org/10.1016/j.chemosphere.2019.125605>
163. Conings, B., Babayigit, A., & Boyen, H.-G. (2019). Fire safety of lead halide perovskite photovoltaics. *ACS Energy Letters*, *4*, 873–878. <https://doi.org/10.1021/acsenergylett.9b00546>
164. (ed US Environmental Protection Agency) (1994).
165. Townsend, T., Y. C. J., Tolaymat, T. (ed University of Florida) (2003).
166. Alsalloum, A. Y., et al. (2020). Low-temperature crystallization enables 21.9% efficient single-crystal MAPbI<sub>3</sub> inverted perovskite solar cells. *ACS Energy Letters*, *5*, 657–662. <https://doi.org/10.1021/acsenergylett.9b02787>
167. Boopathi, K. M., et al. (2017). Solution-processable antimony-based light-absorbing materials beyond lead halide perovskites. *Journal of Materials Chemistry A*, *5*, 20843–20850. <https://doi.org/10.1039/c7ta06679a>
168. Chen, M., et al. (2019). Highly stable and efficient all-inorganic lead-free perovskite solar cells with native-oxide passivation. *Nature Communications*, *10*, 16. <https://doi.org/10.1038/s41467-018-07951-y>
169. Hu, W., et al. (2020). Bulk heterojunction gifts bismuth-based lead-free perovskite solar cells with record efficiency. *Nano Energy*, *68*. <https://doi.org/10.1016/j.nanoen.2019.104362>
170. Ito, N., et al. (2018). Mixed Sn-Ge perovskite for enhanced perovskite solar cell performance in air. *Journal of Physical Chemistry Letters*, *9*, 1682–1688. <https://doi.org/10.1021/acs.jpcllett.8b00275>
171. Jain, S. M., et al. (2018). An effective approach of vapour assisted morphological tailoring for reducing metal defect sites in lead-free, (CH<sub>3</sub>NH<sub>3</sub>)<sub>3</sub>Bi<sub>2</sub>I<sub>9</sub> bismuth-based perovskite solar cells for improved performance and long-term stability. *Nano Energy*, *49*, 614–624. <https://doi.org/10.1016/j.nanoen.2018.05.003>
172. Jeon, N. J., et al. (2018). A fluorene-terminated hole-transporting material for highly efficient and stable perovskite solar cells. *Nature Energy*, *3*, 682–689. <https://doi.org/10.1038/s41560-018-0200-6>
173. Llanos, M., Yekani, R., Demopoulos, G. P., & Basu, N. (2020). Alternatives assessment of perovskite solar cell materials and their methods of fabrication. *Renewable and Sustainable Energy Reviews*, *133*. <https://doi.org/10.1016/j.rser.2020.110207>
174. Lyu, M., et al. (2016). Highly compact and uniform CH<sub>3</sub>NH<sub>3</sub>Sn<sub>0.5</sub>Pb<sub>0.5</sub>I<sub>3</sub> films for efficient panchromatic planar perovskite solar cells. *Science Bulletin*, *61*, 1558–1562. <https://doi.org/10.1007/s11434-016-1147-2>
175. Qiu, J., Xia, Y., Chen, Y., & Huang, W. (2019). Management of crystallization kinetics for efficient and stable low-dimensional Ruddlesden-Popper (IDRP) lead-free perovskite solar cells. *Advanced Science (Weinh)*, *6*, 1800793. <https://doi.org/10.1002/advs.201800793>
176. Singh, A., et al. (2018). Photovoltaic performance of vapor-assisted solution-processed layer polymorph of Cs<sub>3</sub>Sb<sub>2</sub>I<sub>9</sub>. *ACS Applied Materials & Interfaces*, *10*, 2566–2573. <https://doi.org/10.1021/acsmi.7b16349>
177. Li, Z., et al. (2021). Sulfonated graphene aerogels enable safe-to-use flexible perovskite solar modules. *Advanced Energy Materials*, *12*. <https://doi.org/10.1002/aenm.202103236>
178. Li, X., et al. (2021). On-device lead-absorbing tapes for sustainable perovskite solar cells. *Nature Sustainability*, *4*, 1038–1041. <https://doi.org/10.1038/s41893-021-00789-1>
179. Jiang, Y., et al. (2019). Reduction of lead leakage from damaged lead halide perovskite solar modules using self-healing polymer-based encapsulation. *Nature Energy*, *4*, 585–593. <https://doi.org/10.1038/s41560-019-0406-2>
180. Li, X., et al. (2020). On-device lead sequestration for perovskite solar cells. *Nature*, *578*, 555–558. <https://doi.org/10.1038/s41586-020-2001-x>